Theor Chem Acc (1999) 102:377–384
DOI 10.1007/s002149800m96

Theoretical
Chemistry Accounts

Regular article

Acetylene-insertion reactions into Pt(II)—H and Pt(II)—SiH_3 bonds. An ab initio MO study and analysis based on the vibronic coupling model*

Manabu Sugimoto, Ichiro Yamasaki, Nobuteru Mizoe, Masaharu Anzai, Shigeyoshi Sakaki

Department of Applied Chemistry and Biochemistry, Faculty of Engineering, Kumamoto University, Kurokami, Kumamoto 860-8555, Japan

Received: 13 August 1998 / Accepted: 2 September 1998 / Published online: 15 February 1999

Abstract. Acetylene insertion into Pt(II)—H and Pt(II)—SiH_3 bonds of $PtH(SiH_3)(PH_3)$ was investigated using ab initio molecular orbital and Møller-Plesset perturbation theory methods. The insertion into Pt—H was predicted to proceed with a smaller activation energy ($E_a = 12.8$ kcal/mol) than that into Pt—SiH_3 ($E_a = 20.9$ kcal/mol). The reaction energy (ΔE) of the insertion into Pt—H is 10 kcal/mol smaller than that for the insertion into Pt—SiH_3, which reflects differences in bond energies between C—H and C—Si and between Pt—H and Pt—SiH_3. A comparison with ethylene insertion revealed that the acetylene insertion occurs more easily, and the latter reaction is more exothermic. A simple vibronic coupling model combined with Toyozawa's interaction mode analysis was used to examine interesting differences in E_a and ΔE between insertions into Pt—H and Pt—SiH_3, and between acetylene and ethylene insertions. This analysis suggests that the factors determining E_a are the stiffness of the Pt—H and Pt—SiH_3 bonds and the vibronic coupling strength of acetylene and ethylene.

Key words: Ab initio molecular orbital methods – Acetylene insertion – Platinum hydride – Platinum silyl – Vibronic coupling – Hydrosilylation

1 Introduction

The insertion reaction of a C—C double or triple bond is one of the elementary steps in transition-metal-catalysed hydrosilylation of olefins and acetylene [1]. The importance of this step was suggested by Chalk and Harrod [2] and by Schroeder and Wrighton [3]: the insertion into a Pt—H bond is a key step in the Chalk-Harrod mechanism [2], while that into a Pt—Si bond is a key step in the modified Chalk-Harrod mechanism [3]. In spite of this importance, theoretical investigation of olefin- and acetylene-insertion reactions has been limited [4–10].

In recent work, we have reported that ethylene insertion preferentially occurs into the Pt—H bond rather than the Pt—Si bond because of the hardness of the latter bond [8, 9]. Also, we clearly concluded that the platinum-catalysed hydrosilylation of ethylene proceeds through the Chalk-Harrod mechanism, and the modified Chalk-Harrod mechanism is difficult because of the much higher activation energy of insertion into Pt—SiH_3 [8]. Compared to ethylene insertion into M(metal)—H and M—Si bonds, the acetylene insertion reaction is expected to occur more easily. For instance, it was theoretically reported that acetylene is easily inserted into Pt—$B(OH)_2$ but ethylene is inserted into it with a much higher barrier [10]. Therefore, a modified Chalk-Harrod mechanism could be possible if acetylene is inserted into Pt—SiH_3. Actually, Tanaka et al. experimentally reported that $PtBr(SiR_3)(PEt_3)_2$ is more reactive than $PtHBr(PEt_3)_2$ for acetylene insertion [11]. In this respect, we thought it would be interesting to investigate theoretically acetylene-insertion reactions into Pt—H and Pt—Si bonds and to estimate their activation barriers.

In this paper, we report a theoretical investigation of acetylene-insertion reactions into Pt—H and Pt—SiH_3 bonds in $PtH(SiH_3)(PH_3)$ which is considered a model of active species for Pt-catalysed hydrosilylation of alkene and alkyne. Hereafter, these reactions will be referred to as Path 1 and Path 2, respectively (Scheme 1).

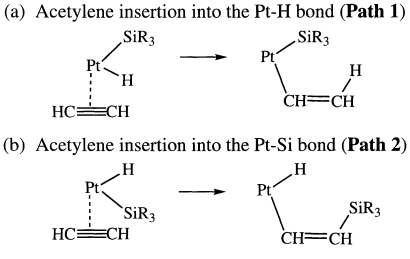

Scheme 1. Reaction paths for acetylene insertions

Since olefin insertion easily occurs via four-coordinate complexes when the central metal takes a d^8 electron

* Contribution to the Kenichi Fukui Memorial Issue

Correspondence to: S. Sakaki or M. Sugimoto

configuration [4, 12, 13], we will examine insertion reactions starting from model complexes of $PtH(SiH_3)(PH_3)(C_2H_2)$ and its isomer. A discussion is also given on the characteristic features of acetylene insertion in comparison with ethylene insertion on the basis of a simple vibronic coupling model [15] combined with Toyozawa's interaction mode analysis [16].

2 Computational details

Electronic structure calculations were carried out with ab initio molecular orbital (MO) method followed by the second-, third-, and fourth-order Møller-Plesset perturbation theories with single, double and quadruple substituents (MP2-MP4SDQ). Geometry optimizations of precursor complexes, transition states (TS) and products involved in acetylene insertion reactions were performed with the MP2 method employing the BS-I basis set defined below. In optimizing TS, no constraint was included, while the structure of PH_3 was fixed to that observed experimentally [17] and rotations along Pt—P and Pt—Si bonds were restricted in other geometries. Energy changes in these reactions were investigated with the MP4SDQ method using a more elaborate basis set (BS-II), where the MP2-optimized geometries were referred to. These calculations were carried out with GAUSSIAN 94 [18].

We used two basis sets as follows. In both basis sets, effective core potentials (ECPs) were adopted to replace core electrons of Pt (up to 4*d*) and P (up to 2*p*) atoms. BS-I consists of (311/311/21) for Pt [19], (21/21) for P [20], (21/21/1) with ECP (up to 2*p*) for Si [20], MIDI-3 set for C [21], (31/1) for a hydride ligand [22] and (31) for the other hydrogen atoms [22]. BS-II was prepared by expanding the BS-I basis set: (541/541/111) for Pt [23], (21/21/1) for P [20], (531111/4211/1) without ECP for Si [22], (721/41/1) for C [22], (311/1) for hydride [24] and (31) for the other H atoms [22].

3 Results and discussion

3.1 Acetylene insertion into the Pt—H bond

Optimized precursor complexes, a transition state (TS) and products of Path 1 are shown in Fig. 1. Energy changes in the reaction are shown in Table 1 where the energy for PCM1b is taken as a standard. We obtained two structures for a precursor complex: in PCM1a, acetylene is almost perpendicular to the P-Pt-Si plane, while in PCM1b it lies on the P-Pt-Si plane. The latter structure is 4.5 kcal/mol more stable than the former, which is consistent with the shorter Pt—C distance in PCM1b than in PCM1a. A binding energy (BE) between $PtH(SiH_3)$ (PH_3) and acetylene defined by

$$BE = E[PtH(SiH_3)(PH_3)] + E[C_2H_2] - E[PtH(SiH_3)(PH_3)(C_2H_2)]$$

was 17.5 kcal/mol.

In the TS along Path 1 (referred to as TS1 in Fig. 1) the Pt—C distance is 0.17 Å shorter than in PCM1b, and 0.06 Å longer than in the initial product (PRD1a; see below). A normal mode analysis showed that the optimized TS had only one imaginary frequency of 811 cm^{-1}. The C—C distance (1.30 Å) of the vinyl group also

Fig. 1. Geometry changes in acetylene insertion into the Pt—H bond of $PtH(SiH_3)(PH_3)$

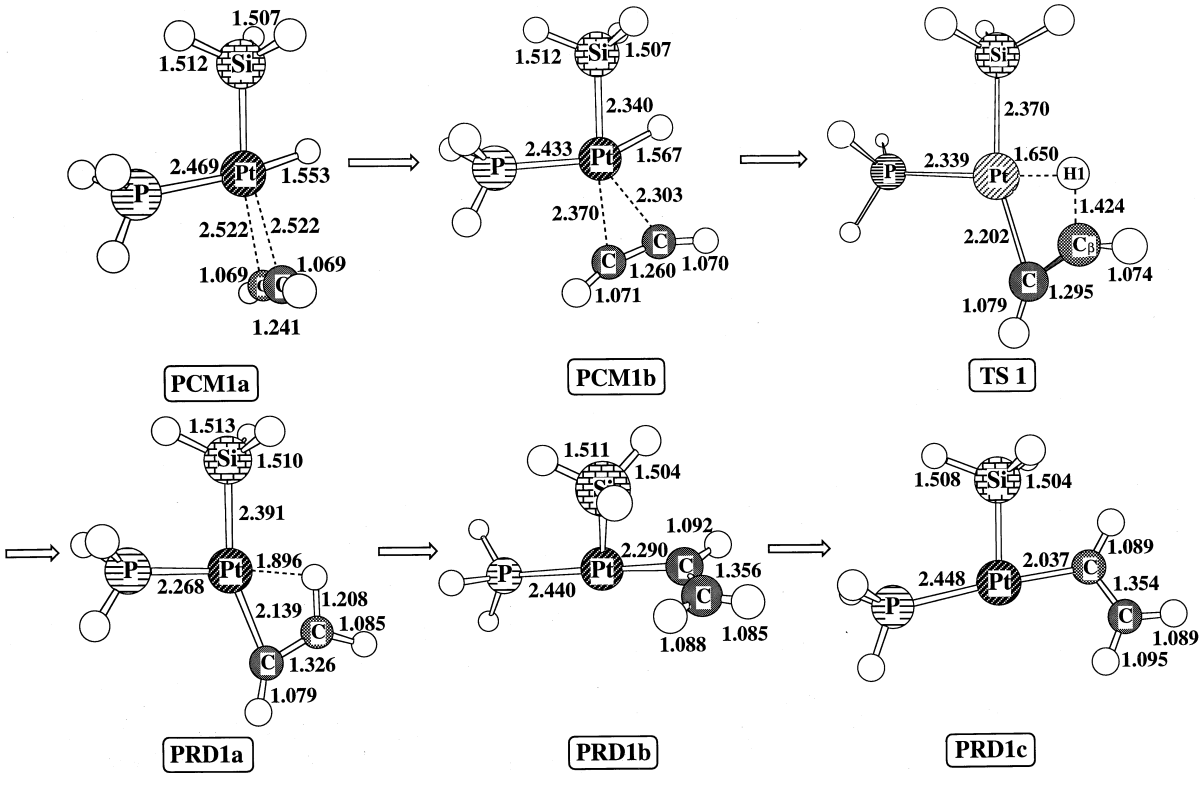

Table 1. Energy changes in the acetylene-insertion reaction into the Pt—H bond of $PtH(SiH_3)(PH_3)$ in kcal/mol. PCM1b is taken as a reference. See also Fig. 1 defining notations for structures

Method	PCM1a	PCM1b	TS1	PRD1a	PRD1b	PRD1c
RHF[a]	−0.4	0.0	5.8	−0.6	−31.9	−31.5
MP2	7.2	0.0	14.3	12.4	−16.5	−13.9
MP3	3.0	0.0	10.7	6.1	−24.5	−23.0
MP4(DQ)	4.3	0.0	12.6	8.6	−22.0	−20.2
MP4(SDQ)	4.5	0.0	12.8	8.9	−21.4	−19.6

[a] RHF, restricted Hartree-Fock

shows that a triple-bond character for the C—C bond is maintained and it is shorter than the typical C—C double bond (1.33–1.36 Å in PRD1a–PRD1c). The Pt—H bond is elongated by only 0.08 Å at TS1, accompanied by the approach of the hydride ligand to the C^{β} atom. The activation energy (E_a) was calculated to be 12.8 kcal/mol (MP4SDQ), which is almost the same as that for the corresponding ethylene insertion reaction (12.7 kcal/mol) reported previously [8].

In the product, three isomers were optimized, as shown by PRD1a–c (Fig. 1). PRD1a is considered as the initial product directly formed from TS1. Interestingly, PRD1a involves an agostic interaction: the $C—H^1$ distance of 1.21 Å is much longer than the usual sp^2-C—H bond, and $Pt—H^1$ has a length of 1.90 Å, which indicates that some bonding interaction exists between Pt and H^1. In PRD1b and PRD1c, the silyl and vinyl ligands take the *cis*-position to each other, suggesting that the subsequent reductive-elimination reactions of vinylsilane would occur from PRD1b and PRD1c. PRD1a is ca. 30 kcal/mol less stable than PRD1b and PRD1c, because the *trans* influence of SiH_3 is stronger than that of PH_3 [25, 26]. The energy difference is very small between PRD1b and PRD1c. In both PRD1b and PRD1c, a hydrogen bound to C^{β} is too far from Pt to form an agostic interaction with Pt. Therefore, rotational motion about the Pt—C bond is expected to occur easily, leading to a small energy difference between them. PRD1b is the most stable product and is 21.4 kcal/mol more stable than PCM1b. In the ethylene insertion reaction, similar products were reported, but the exothermicity for the most stable product was 9.3 kcal/mol. This is about 50% of that for the acetylene insertion reaction.

Since PRD1a produced by the insertion is much less stable than PRD1b and PRD1c, the isomerization would occur from PRD1a to PRD1b and to PRD1c. In the ethylene insertion reaction, the TS for the isomerization of the products was successfully optimized. The activation barrier of this process was calculated to be 10 kcal/mol. In the acetylene insertion (Path 1) investigated here, any efforts to optimize the corresponding TS led to an unsatisfactory result. Considering that PRD1b and PRD1c are ca. 30 kcal/mol more stable than PRD1a, it is reasonable to suggest that isomerization from PRD1a to PRD1b or PRD1c might occur with a very low barrier.

3.2 Acetylene insertion into the Pt—SiH_3 bond

Figure 2 summarizes optimized structures of the reactants, the TS and products involved in Path 2. Structures of two precursor complexes, PCM2a and PCM2b, are essentially similar to PCM1a and PCM1b, respectively. A planar complex (PCM2b) is 5.8 kcal/mol more stable than a non-planar one (PCM2a), as shown in Table 2.

In TS2, the Pt—C bond is shorter than that in TS1 by 0.14 Å. TS2 has one vibrational mode whose frequency is imaginary ($159\,cm^{-1}$). The C—C bond distance of 1.37 Å is almost the same as the usual C—C double bond distance. The $Si—C^{\beta}$ distance (1.94 Å) suggests that this bond is almost formed since it is similar in length to those of PRD2a–2e. The Pt—Si bond is 2.65 Å indicating that this bond has been broken. All these features suggest that TS2 is considered product-like. Consistent with this late TS, the E_a of this process (20.9 kcal/mol) is 8 kcal/mol higher than that of Path 1.

Five isomers (PRD2a–e) were optimized as products of the insertion reaction. Since PRD2a and PRD2c are 14 and 10 kcal/mol more stable than PRD2d and PRD2e, respectively, and since the rotation about the C—C double bond usually requires much large E_a, PRD2d and PRD2e seem less important as insertion products, but they were calculated here to estimate the strength of agostic interaction. They are *trans* isomers of PRD2a and PRD2c, respectively. Judging from the short Pt—H distance, agostic interaction works in PRD2a and PRD2c in contrast to PRD1c. Energy differences between products with and without the agostic interaction (for instance PRD2c and PRD2e) give an estimated interaction energy of 10 kcal/mol. This energy is reflected in an energy difference (11 kcal/mol) between PRD2b and PRD2c. Interestingly, the agostic interaction of the ethylene-insertion product was estimated to be 5 kcal/mol, which is 50% of the acetylene-insertion product. It is well known that this interaction arises from charge transfer from hydrogen to the unoccupied 5*d* orbital of Pt [27]. Since the vinyl group is more electronegative than the ethyl group, as will be shown below, the Pt atom would be more electron-deficient in the acetylene-insertion product, leading to a stronger agostic interaction.

The TS (iso-TS2) for isomerization between PRD2a and PRD2b (or PRD2c) was optimized as shown in Fig. 2. The $CH{=}CHSiH_3$ group is at a position almost *trans* to PH_3. The activation barrier was calculated to be 17.2 kcal/mol which is similar to that of the corresponding isomerization among ethylene-insertion products [8].

3.3 Comparison of acetylene-insertion reactions into Pt—H and Pt—SiH_3 bonds

E_a seems to be correlated to the degree of structural deformation of the $Pt—SiH_3$ bond of $PtH(SiH_3)$ (PH_3) moiety in TS (Fig. 1 and 2). For instance, the $Pt—SiH_3$ bond significantly distorts in TS2 but the Pt—H bond moderately distorts in TS1. In order to quantify the distortion of this moiety, we define the distortion energy ΔE_{dist}, as follows:

$$\Delta E_{dist} = E_{TS} - E_{react} \quad , \tag{1}$$

where E_{TS} and E_{react} are energies of a fragment (e.g. $PtH(SiH_3)(PH_3)$ moiety) in TS and in the precursor

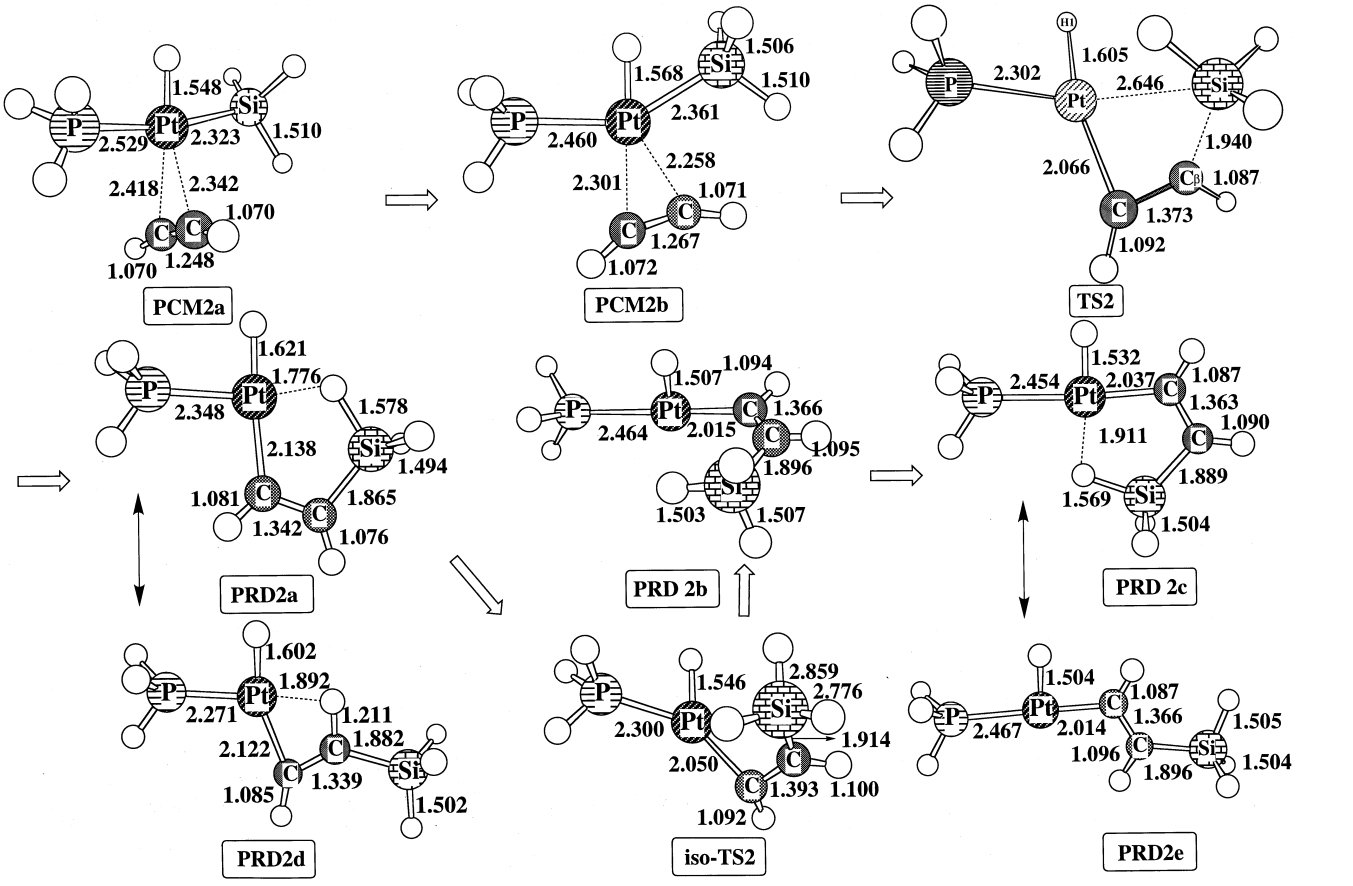

Fig. 2. Geometry changes in acetylene insertion into the Pt—SiH_3 bond of $PtH(SiH_3)(PH_3)$

Table 2. Energy changes in the acetylene-insertion reaction into the Pt—SiH_3 bond of $PtH(SiH_3)(PH_3)$ in kcal/mol. PCM2b is taken as a reference. See also Fig. 2 defining notations for structures

Method	PCM2a	PCM2b	TS2	PRD2a	PRD2b	PRD2c
RHF	2.1	0.0	16.0	−11.9	−17.0	−21.5
MP2	8.7	0.0	23.8	8.9	5.2	−6.7
MP3	5.2	0.0	19.7	−1.1	−6.6	−15.9
MP4(DQ)	6.0	0.0	21.7	2.9	−2.1	−12.1
MP4(SDQ)	5.8	0.0	20.9	3.5	−1.0	−11.7

complex (PCM1a and PCM2a), respectively. As shown in Table 3, ΔE_{dist} of the $PtH(SiH_3)(PH_3)$ moiety is 2.9 and 39.6 kcal/mol for Path 1 and Path 2, respectively, while ΔE_{dist} of the acetylene moiety is 23.1 and 51.3 kcal/mol for Path 1 and Path 2, respectively. Thus, TS1 may be classified as an early TS. The interaction energy ($\Delta E_{int} = E_a - \Delta E_{dist}$), which is equivalent to the binding energy between two distorted moieties in TS, is −13.2 kcal/mol, and compensates the destabilization due to the distortion energies. For Path 2, the total distortion energy is 90.9 kcal/mol which is about 3.5 times larger than that for Path 1. The binding energy between the distorted $PtH(SiH_3)(PH_3)$ and acetylene moieties is 70.0 kcal/mol. These large distortion and binding energies of TS2 means that TS2 is more product-like. Therefore, it should be concluded that the larger distortion energy for Path 2 is the main reason for the

Table 3. Distortion energies (ΔE_{dist}) of $PtH(SiH_3)(PH_3)$ and acetylene moieties in transition-state geometries, activation energies (E_a) for acetylene insertion and interaction energies (ΔE_{int}) (kcal/mol)

	ΔE_{dist}			E_a	ΔE_{int}
	Pt	Acetylene	Total		
Path 1	2.9	23.1	26.0	12.8	−13.2
Path 2	39.6	51.3	90.9	20.9	−70.0

higher activation energy. A similar difference between the insertions into Pt—H and Pt—SiH_3 was reported for the ethylene-insertion reaction investigated previously [8]. This difference is explained as follows: the SiH_3 ligand has such a strongly directional sp^3 valence orbital that SiH_3 should tilt its orientation toward acetylene to cause a large distortion.

The reaction energy (exothermicity) for Path 1 was calculated to be −21.4 kcal/mol and that for Path 2 −11.7 kcal/mol. This difference can be explained on the basis of the energy gain by bond formation and energy loss by bond scission. We calculated the Pt—H bond energy by considering the following reactions:

$$Pt(PH_3)_2 + H_2 \rightarrow \text{cis-}PtH_2(PH_3)_2 \ , \quad (2)$$

$$H_2 \rightarrow 2{\cdot}H \ . \quad (3)$$

The Pt—SiH_3 bond energy was evaluated with Eqs. (4) and (5) and with the estimated Pt—H bond energy:

Table 4. Bond energies for Pt—H, Pt—SiH_3, Pt-vinyl, Pt-ethyl, vinyl-H (C—H) and vinyl-SiH_3 (C—SiH_3) bonds (kcal/mol)

Method	D(Pt—H)	D(Pt—SiH_3)	D(Pt-vinyl)	D(Pt-ethyl)	D(C—H)	D(C—SiH_3)
RHF	45.7	39.7	26.6	12.5	89.3	70.8
MP2	59.5	58.0	58.1	42.6	108.5	96.8
MP3	61.5	55.1	51.3	36.9	107.9	93.1
MP4(DQ)	61.6	55.7	50.5	36.4	108.0	92.2
MP4(SDQ)	61.2	56.0	50.4	37.1	107.3	91.8

$$Pt(PH_3)_2 + H - SiH_3 \rightarrow \text{cis-}PtH(SiH_3)(PH_3)_2 \ , \quad (4)$$

$$H{-}SiH_3 \rightarrow \cdot H + \cdot SiH_3 \ . \quad (5)$$

The Pt-vinyl bond energy was evaluated with the Pt—SiH_3 bond energy and Eqs. (6) and (7):

$$\text{cis-}Pt(SiH_3)(CH{=}CH_2)(PH_3)_2 \rightarrow Pt(PH_3)_2 + CH_2{=}CHSiH_3 \ , \quad (6)$$

$$CH_2{=}CHSiH_3 \rightarrow \cdot SiH_3 + \cdot CH{=}CH_2 \ . \quad (7)$$

The C—H bond energy was simply calculated using

$$CH_2{=}CH_2 \rightarrow \cdot H + \cdot CH{=}CH_2. \quad (8)$$

Table 4 indicates that, assuming that the Pt-vinyl bond is constant (50.4 kcal/mol) independent of $\cdot CH{=}CH_2$ and $\cdot CH{=}CH{-}SiH_3$, a difference in energy loss between Pt—H and Pt—SiH_3 arises from Pt—H and Pt—SiH_3 bond energies, from which the insertion into Pt—H is 5 kcal/mol more favourable than that into Pt—SiH_3. The difference in energy gain between Pt—H and Pt—SiH_3 corresponds to the difference between the vinyl-H and vinyl-SiH_3 bond energies for which the insertion into Pt—H is 16 kcal/mol more favourable than that into Pt—SiH_3. The sum of the difference is 10.3 kcal/mol, which explains the difference in exothermicity (7.9 kcal/mol) between Path 1 and Path 2. From the above discussion, it can be concluded that the larger exothermicity of Path 1 may be attributed to the fact that the vinyl-H bond is stronger than the vinyl-SiH_3 bond.

Population changes estimated with the natural bond orbital (NBO) analysis [28] reveal two interesting features. As shown in Fig. 3, the electron population of the acetylene increases more rapidly in Path 2 than in Path 1: 0.32 electrons are transferred to acetylene in TS1 and 0.47 electrons in PRD1a, while acetylene accepts 0.71 electrons in TS2. This difference between TS1 and TS2

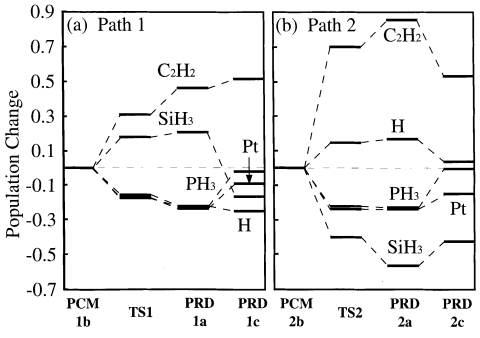

Fig. 3a,b. Electron population changes in acetylene insertions calculated with the NBO analysis: **a** insertion into the Pt—H bond, **b** insertion into the Pt—Si bond

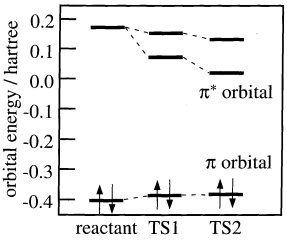

Fig. 4. π and π* orbital energies of acetylene in the optimized, TS1 and TS2 geometries

can be related to orbital energy levels of acetylene shown in Fig. 4 where the orbitals are given for the equilibrium structure and the distorted one taken in TS1 and TS2. We see that the energy lowering of one of the two π^* orbitals, which should be responsible for the charge transfer mentioned above, is more drastic in TS2 than in TS1. Thus, the structural distortion is found to enhance the electron-withdrawing ability of acetylene through the stabilization of its π^* orbital. The other interesting finding is that, in both reaction paths, the electron population increases in a similar extent for both H in Path 1 and for SiH_3 in Path 2. This result implies that dative bonds of H (Path 1) and SiH_3 (Path 2) weaken as the reaction proceeds. The bond weakening of Pt—H (Path 1) and Pt—SiH_3 (Path 2) is easily understood in terms of the Pt-vinyl bond formation at a position *trans* to either H (Path 1) or SiH_3 (Path 2). Consistent with this understanding, the H population decreases again upon going from PRD2a to PRD2c and the silyl population decreases upon going from PRD1a to PRD1c since the *trans* position of SiH_3 and H are empty in PRD1c and PRD2c, respectively.

3.4 Vibronic coupling model analysis on acetylene- and ethylene-insertion reactions

Table 5 shows the activation and reaction energies for acetylene and ethylene insertions into Pt—H and Pt—SiH_3 bonds where we have optimized TS for acetylene insertions with constraints similar to those adopted in our previous study[1] [8, 9]. In these reactions, insertion into the Pt—H bond is preferential to insertion into Pt—SiH_3. Table 5 also suggests that Path 1 is more exothermic than Path 2, and that acetylene insertion is more exothermic than the ethylene insertion in both

[1] Pt, two C and hydride (or Si) atoms were placed on the same plane for TS1 and TS2. In Ref. [8] geometries were optimized with the Hartree-Fock method, while the present study employed the MP2 method. Since the electron correlation effect is expected to be small in such an insertion reaction as reported in Ref. [8] both methods would give very similar structures.

Table 5. Activation energy (E_a) and reaction energy (ΔE) (for a product whose conformation is similar to PRD1c) for acetylene- and ethylene-insertion reactions into Pt—H (Path 1) and Pt—SiH_3 (Path 2) bonds and their analysis based on the two-electron/two-orbital vibronic coupling model. Transition state geometry was optimized with some constraints. See the Footnote 1

	E_a (kcal/mol)	ΔE (kcal/mol)	λ (kcal/mol)	V_0 (kcal/mol)	Q_1^*	ε_b (hartree)	α
Acetylene insertion							
Path 1	11.9	−19.6	3.06	−14.9	4.88	0.512	0.956
Path 2	29.8	−11.7	1.39	−10.7	7.72	0.505	0.967
Ethylene insertion							
Path 1	12.7	−7.7	1.35	− 6.8	5.04	0.489	0.978
Path 2	44.1	5.6	0.62	5.8	−9.39	0.482	1.020

paths. In addition, we see that E_a is nearly equal for acetylene and ethylene insertions when they proceed via Path 1, while the acetylene insertion occurs more easily in Path 2 than the ethylene insertion.

We analysed these reactions using the model Hamiltonian [15]

$$H = H_a + H_b + H_{\text{int}} \ . \tag{9}$$

The subscripts a and b denote $PtH(SiH_3)(PH_3)$ and acetylene (or ethylene), respectively, and the last term represents the interaction between them. We consider a two-electron/two-orbital model in which the highest occupied molecular orbital (HOMO) of $PtH(SiH_3)$-(PH_3) and one π^* orbital of acetylene (or ethylene) are taken into account. These orbitals are illustrated in Scheme 2. In the harmonic approximation, the first and second terms may be given by

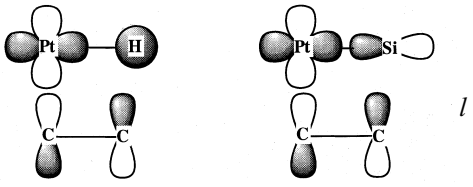

Scheme 2. Molecular orbitals considered in the vibronic coupling model

$$H_a = \varepsilon_a a^\dagger a + \frac{1}{2} k_a q_a^2 \ , \tag{10}$$

$$H_b = \varepsilon_b b^\dagger b + \frac{1}{2} k_b q_b^2 \ , \tag{11}$$

where q_a and q_b are displacements from the equilibrium position in deformation modes which are not necessarily normal modes. $a^\dagger$ and a are creation and annihilation operators for the HOMO of the $PtH(SiH_3)(PH_3)$ moiety. $b^\dagger$ and b are those for the π^* orbital of acetylene or ethylene. We consider the interaction between these two moieties represented as

$$H_{\text{int}} = t(a^\dagger b + b^\dagger a) + \gamma_a a^\dagger a q_a + \gamma_b b^\dagger b q_b \ , \tag{12}$$

where t and γ are the resonance integral and vibronic coupling strength. Strictly speaking, the coupling considered here is the Herzberg-Teller vibronic coupling which is a correction for the crude *adiabatic* approximation leading to the Born-Oppenheimer *adiabatic* approximation [29]. Here we investigate an adiabatic potential based on reactant orbitals $|a\rangle$ and $|b\rangle$ at $q_a = 0$ and $q_b = 0$ (equilibrium structures), respectively. Such a model is also known as a small-polaron-type model in electron transfer studies [30]. Using the linear combination of atomic orbitals (LCAO) approximation, the adiabatic potential U is represented by

$$U = \frac{1}{2} k_a q_a^2 + \frac{1}{2} k_b q_b^2 + \left[(\varepsilon_b + \gamma_a q_a + \gamma_b q_b) - \sqrt{(\varepsilon_b - \gamma_a q_a + \gamma_b q_b)^2 + 4t^2} \right] \ , \tag{13}$$

where ε_a is set to zero for convenience. If the displacement is small enough, the second term in the square bracket in Eq. (13) may be approximated as follows:

$$\sqrt{(\varepsilon_b - \gamma_a q_a + \gamma_b q_b)^2 + 4t^2} \approx \sqrt{\varepsilon_b^2 + 4t^2} - \frac{\gamma_a \varepsilon_b}{\sqrt{\varepsilon_b^2 + 4t^2}} q_a + \frac{\gamma_b \varepsilon_b}{\sqrt{\varepsilon_b^2 + 4t^2}} q_b \ . \tag{14}$$

Then, the adiabatic potential for the final state, corresponding to the product, results in

$$U = \frac{1}{2} k_a q_a^2 + \frac{1}{2} k_b q_b^2 + (1 + \alpha)\gamma_a q_a + (1 - \alpha)\gamma_b q_b + V_0 \ , \tag{15}$$

where

$$V_0 = \frac{\alpha - 1}{\alpha} \varepsilon_b \ , \tag{16}$$

$$\alpha = \frac{\varepsilon_b}{\sqrt{\varepsilon_b^2 + 4t^2}} \ . \tag{17}$$

Following Toyozawa and Inoue [16], we use a transformation defined by

$$Q_1 = \frac{\gamma_a (1 + \alpha)}{\lambda} q_a + \frac{\gamma_b (1 - \alpha)}{\lambda} q_b \ , \tag{18-a}$$

$$Q_2 = -\frac{\gamma_b (1 - \alpha)}{\lambda} \left(\frac{k_a}{k_b} \right)^{1/2} q_a + \frac{\gamma_a (1 + \alpha)}{\lambda} \left(\frac{k_b}{k_a} \right)^{1/2} q_b \ . \tag{18-b}$$

Using Q_1 and Q_2, U can be expressed as

$$U = \frac{1}{2}(Q_1 + \lambda)^2 + \frac{1}{2}Q_2^2 + V_0 - \frac{1}{2}\lambda^2 \quad . \tag{19}$$

Interestingly Q_1 corresponds to the minimum energy path. The λ is a displacement along the interaction mode Q_1 caused by H_{int}, and is given by

$$\lambda = \left[\frac{\gamma_a^2}{k_a}(1+\alpha)^2 + \frac{\gamma_b^2}{k_b}(1-\alpha)^2\right]^{1/2} \quad . \tag{20}$$

In the initial state, the adiabatic potential is expressed as

$$U_0 = \frac{1}{2}Q_1^2 + \frac{1}{2}Q_2^2 \quad . \tag{21}$$

The TS in this model corresponds to the crossing point of U and U_0. Thus, a coordinate $Q_1^{\neq}$ representing the TS, the activation energy E_a, and the reaction energy ΔE are represented by

$$Q_1^{\neq} = -\frac{V_0}{\lambda} \quad , \tag{22}$$

$$E_a = \frac{V_0^2}{2\lambda^2} \quad , \tag{23}$$

$$\Delta E = V_0 - \frac{1}{2}\lambda^2 \quad , \tag{24}$$

respectively. Even if many vibrational modes contribute to the reaction, we can always define a single interaction mode using the transformation defined by Eq. (18) as long as the modes couple with those of another moiety very weakly. Using Eqs. (22–24), λ, V_0, $Q_1^{\neq}$ and α can be evaluated with E_a, ΔE and ε_b values from ab initio MO calculations (Table 5). In estimating ε_b, orbital energies of the HOMO of $PtH(SiH_3)(PH_3)$ and the lowest unoccupied molecular orbital (LUMO) (π^*) of acetylene (or ethylene) were used.

Table 5 shows that $Q_1^{\neq}$ in Path 1 is smaller than that in Path 2 for acetylene and ethylene insertions. This means that the TS structure in Path 1 is more reactant-like. A difference in λ is dominant to that in $Q_1^{\neq}$ though V_0 also contributes to some extent. The γ_a^2/k_a term in Eq. (20) mainly determines λ because α is expected to give a similar contribution (see Eq. 20 and Table 5). It is reasonable to consider that the deformation mode of the Pt—SiH_3 bond is stiffer than that of the Pt—H bond, i.e. $k_a(\text{Pt—SiH}_3) \gg k_a(\text{Pt—H})$. This is because the sp^3 valence orbitals of SiH_3 is expected to be directional unlike the 1s orbital of H (hydride), as was pointed out in Sect. 3.3. Thus, the stiffness of the bond to be broken explains a difference in E_a on the basis of Eq. (23).

With respect to ΔE, the contribution from structural relaxation ($-\lambda^2/2$) is estimated to be -4.7 kcal/mol, and that from orbital mixing, i.e. an electronic factor V_0, is -14.9 kcal/mol for the product in Path 1. Comparing acetylene- and ethylene-insertion reactions into the Pt—H bond, larger exothermicity also results from a larger contribution of V_0: the contribution from the vibronic coupling is only -4.7 kcal/mol for acetylene and -0.9 kcal/mol for ethylene. Therefore it may be concluded that the bonding interaction between $PtH(SiH_3)(PH_3)$ and acetylene (or ethylene), whose strength is represented by V_0, determines the exothermicity of the reaction. In Sect. 3c, we have pointed out that a difference in exothermicity can be related to bond energies. As is shown in Table 4, the energy destabilization of 61.2 kcal/mol in Path 1 is necessary to break the Pt—H bond, which is compensated by the formation of a C—H bond (107 kcal/mol) and either a Pt-vinyl (50 kcal/mol) or Pt-ethyl (37 kcal/mol) bond. The difference in bond energies for Pt-vinyl and Pt-ethyl bonds is 13 kcal/mol, which corresponds to the difference in exothermicity between acetylene- and ethylene-inserted products (12 kcal/mol).

It is interesting to note that the E_a for acetylene is very close to that for ethylene when the insertion occurs via Path 1. This similarity is fortuitous since both λ and V_0 are different for these molecules. Although V_0 is larger in magnitude for acetylene, a larger λ compensates the resultant destabilization of TS. This trend is also true for Path 2: for ethylene, V_0 is 56% of that for acetylene, but λ decreases to 39% of that for the latter. In these cases, a force constant of a deformation mode q_b does not explain a difference in λ: the elongation of the C—C bond occurs in insertion reactions and would be included in q_b. The k_b for acetylene would be larger than that for ethylene because the C—C triple bond is stiffer than the C—C double bond. If this factor is important, the ethylene insertion would proceed with a lower activation energy, which is inconsistent with the calculated results. Therefore, we suggest that the vibronic coupling strength, γ_b, is a dominant factor for λ rather than k_b, and that γ_b is larger in acetylene insertion.

The parameter γ may be interpreted as a measure of a response of a reactant to the interaction due to another molecule. Since the orbital mixing is accompanied by a flow of electrons from the Pt moiety to acetylene or ethylene, it is reasonable to consider that a value of γ would reflect such a geometric response to charge transfer. Actually, the NBO analysis shows that the electron population on acetylene largely increases by 0.70 e on going from PCM2b to TS2, while that on ethylene increases by 0.58 e.

In order to examine this more closely, we estimated the structural relaxation energies of acetylene and ethylene after one electron is attached. Figure 5 shows schematic potential energy curves for these molecules where the equilibrium structures of neutral and anion states were optimized with the MP2 method employing BS-I, followed by the MP4(SDQ)/BS-II calculation to estimate energy changes. As seen in Fig. 5, the anionization energy of acetylene is 28 kcal/mol larger than that of ethylene when structural relaxation is not allowed. This means that charge transfer from the Pt

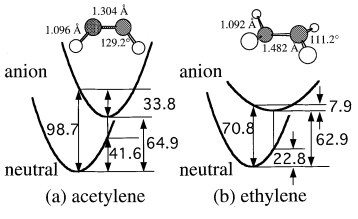

Fig. 5a,b. Schematic potential energy curves for acetylene, ethylene and their anions

moiety to acetylene is unfavourable without relaxation. When the geometry is relaxed after anionization, the acetylene anion becomes lower in energy than ethylene anion. Therefore, the potential curve of the acetylene anion is expected to show a steeper gradient at the equilibrium structure of the neutral state than that for the ethylene anion. This seems to support the fact that γ is larger in acetylene, namely it is more susceptible to charge transfer than ethylene.

4 Conclusions

Acetylene insertion reactions into Pt—H and Pt—SiH_3 bonds of $PtH(SiH_3)(PH_3)$ were studied with ab initio MO/MP2-MP4(SDQ) methods. The insertion into the Pt—H bond was found to proceed with a lower activation barrier than that into the Pt—SiH_3 bond. This result is similar to the ethylene-insertion reaction studied previously [8, 9]. The higher barrier of insertion into Pt—Si may be interpreted in terms of the fact that this bond must be distorted in the TS to tilt the SiH_3 group toward acetylene. This is due to the strongly directional sp^3 orbital of SiH_3. These insertion reactions were also found to be exothermic, and the reaction energy for the insertion into Pt—H was 9.7 kcal/mol larger than that into Pt—Si. We have shown that calculated bond energies can be related to a difference in exothermicity.

We analysed E_a and ΔE calculated with ab initio methods on the basis of a simple vibronic coupling model combined with Toyozawa's interaction mode analysis. These quantities and the TS geometry were expressed with a displacement (λ) along the interaction mode (Q_1) and electronic factors (V_0 and ε_b). The height of the activation barrier is dependent on the ratio V_0/λ for which a difference between insertions into Pt—H and Pt—Si mainly originates from λ. Consistent with the above conclusion, difficulty of the insertion into the Pt—Si bond arises from the stiffness of this bond: a larger force constant of a bond-distortion mode results in smaller λ and, thereby, larger E_a.

The model also successfully explained differences in energetics for acetylene and ethylene insertions into the Pt—H bond. A dominant contribution to ΔE results from the electronic factor V_0, which may be related to bond energies. E_a was found to be similar for acetylene and ethylene because larger V_0 for acetylene is compensated by larger λ. This leads to similar TS geometry for these reactants and results in almost the same E_a. A difference in λ mainly reflects the difference in vibronic coupling strength, and ab initio calculations suggest that the vibronic coupling is stronger in acetylene than in ethylene.

Acknowledgements. This work was supported in part by the Ministry of Education, Culture, Sport and Science through Grants-in-Aid for Scientific Research for the Priority Area of Inter-element Chemistry (Grant 09239105). Some calculations were carried out using the SP2 and HSP computers at the Institute for Molecular Science, Okazaki.

References

1. As a review, see e.g. Ojima I (1989) In: Patai S, Rappoport Z (eds) The chemistry of organic silicon compounds. Wiley, New York, Chap. 25, p 1479
2. Chalk AJ, Harrod JF (1965) J Am Chem Soc 87: 16
3. Schroeder MA, Wrighton JF (1977) J Organometa Chem 128: 345
4. Thern DL, Hoffmann R (1978) J Am Chem Soc 100: 2079
5. Koga N, Obara S, Kitaura K, Morokuma K (1985) J Am Chem Soc 107: 7109
6. Daniel C, Koga N, Han J, Fu XY, Morokuma K (1988) J Am Chem Soc 110: 3773
7. Koga N, Jin SQ, Morokuma K (1988) J Am Chem Soc 110: 3417
8. Sakaki S, Mizoe N, Sugimoto M (1998) Organometallics 17: 2510
9. Sakaki S, Ogawa M, Musashi Y, Arai T (1994) J Am Chem Soc 116: 7258
10. Cui Q, Musaev DG, Morokuma K (1997) Organometallics 16: 1355
11. Yamashita H, Tanaka M, Goto M (1993) Organometallics 12: 988
12. (a) Clark HC, Kurosawa H (1978) J Am Chem Soc 100: 2079; (b) Clark HC, Jablonski CR, Halpern J, Mantovani A, Well TA (1974) Inorg Chem 13: 1541; (c) Clark HC, Jablonski CR (1974) Inorg Chem 13: 2213; (d) Clark HC, Wong CS (1974) J Am Chem Soc 96: 7213; (e) Clark HC, Jablonski CR, Wong CS (1975) Inorg Chem 14: 1332
13. Ben-David Y, Portnoy M, Gozin M, Milstein D (1992) Organometallics 11: 1995
14. Ermer SP, Struck GE, Bitler SR, Richards R, Bau RR, Flood TC (1993) Organometallics 12: 2634
15. Wong KY, Schatz PN (1981) Prog Inorg Chem 28: 369
16. Toyozawa Y, Inoue M (1966) J Phys Soc Jpn 21: 1663
17. Herzberg G (1967) Molecular spectra and molecular structure, Vol 3. Van Nostrand, Princeton N.J., p 610
18. Frisch MJ, Trucks GW, Schlegel HB, Gill PMW, Johnson BG, Robb MA, Cheeseman JR, Keith TA, Petersson GA, Montgomery JA, Raghavachari K, Al-Laham MA, Zakrzewski VG, Ortiz JV, Foresman JB, Cioslowski J, Stefanov BB, Nanayakkara A, Challacombe M, Peng CY, Ayala PY, Chen W, Wong MW, Andres JL, Replogle ES, Gomperts R, Martin RL, Fox DJ, Binkley JS, Defrees DJ, Baker J, Stewart JP, Head-Gordon M, Gonzalez C, Pople JA (1995) Gaussian 94. Gaussian Inc., Pittsburgh, Pa.
19. Hay PJ, Wadt WR (1985) J Chem Phys 82: 299
20. Wadt WR, Hay PJ (1985) J Chem Phys 82: 284
21. Huzinaga S, Andzelm J, Klobukowski M, Radzio-Andzelm E, Sakai Y, Tatewaki H (1984) Gaussian basis sets for molecular calculations. Elsevier, Amsterdam
22. Dunning TH, Hay PJ (1977) In: Schaeffer HF (ed) Methods of electronic structure theory. Plenum, New York, p 1
23. Couty M, Hall MB (1996) J Comput Chem 17: 1359
24. Dunning TH (1971) J Chem Phys 55: 716
25. Sakaki S, Mizoe N, Sugimoto M (to be published)
26. Chatt J, Eaborn C, Ibekwe SD, Kapoor PN (1970) J Chem Soc 1343
27. (a) Koga N, Obara S, Morokuma K (1984) J Am Chem Soc 106: 4625; (b) Obara S, Koga N, Morokuma K (1984) J Organometa Chem 270: C33; (c) Koga N, Obara S, Morokuma K (1985) J Am Chem Soc 107: 7109
28. Reed AE, Curtis LA, Weinhold F (1988) Chem Rev 88: 849
29. Azumi T, Matsuzaki K (1977) Photochem Photobiol 25: 315
30. Mikkelsen KV, Ratner MA (1987) Chem Rev 87: 113